

Testing the Wear of Cultivat or Coultersre in Forced with Cemented-Carbide Plates

Anjan Kumar M. U., Amarnath Nayak, Smita Sahoo, Smrutiranjana Ranjan Pradhan

Department of Civil Engineering, NM Institute of Engineering and Technology, Bhubaneswar, Odisha
Department of Civil Engineering, Raajdhani Engineering College, Bhubaneswar, Odisha
Department of Civil Engineering, Aryan Institute of Engineering and Technology Bhubaneswar, Odisha
Department of Civil Engineering, Capital Engineering College, Bhubaneswar, Odisha

ABSTRACT : *Three constructional arrangements of coulters utilized in cultivators were surveyed with respect to their wear opposition in soil. The coulters were introduced on a four-shaft cultivator utilized for development of loamy-sandy soils with moistness ordinary for the mid year season. It was discovered that the measure of thickness decrease of the coulters in the territories with established carbide plates and cushioning welds was lower than that in the base-material zones. It was likewise discovered that the measure of wear of the coulters introduced on the principal cultivator shaft was the most elevated and diminished on the ensuing pillars. The ruling system of the wear of martensitic steel was microcutting and cutting. The cushion welded material was exposed to an unpredictable wear component (overwhelmed by microcutting). The wear component of the solidified carbide plates included trademark stages.*

Keywords: *Abrasive wear; Cultivator coulters; Cemented carbide; Hardfacing; Soil; Boron steels; Martensitic steels; Agriculture;*

INTRODUCTION

Underservice, working parts of tillage tools are subjected to complex influences dependent on their geometry, the tillage conditions, and the physico-chemical condition of soil. The actuality of the problems related to wear and durability of the parts working in soil is determined by the high variability of the service conditions, the observed tendency to introduce new material and constructional solutions, as well as incomplete knowledge about interactions between the working elements and soil abrasiveness. Research on this topic has mostly focused on some selected aspects of the phenomena occurring in the "working element-soil" system. For example, many research studies considered the influence of soil conditions and tillage parameters on the wear of the elements working in soil [1–12]. It was demonstrated that, among other factors, wear intensity and geometry changes of the working elements depend on the moisture content in soil [4,6,10,11], the granulometric composition of soil [1,13,14], or the tillage speed [2]. Research on the cognitive nature was also undertaken, in order to identify the mechanisms of abrasive wear of the materials used for elements working in soil. In this context, boronized steels and steels with a microadditive of boron [15–18], pad-welded materials [19–24] or cemented carbides [25–27], and oxidic ceramics [28–30] were examined as perspective materials for agricultural applications.

In order to describe and estimate the interactions between the working elements and soil, methods based on computer-aided mathematical models, such as discrete element method (DEM) [31–33] and computational fluid dynamics (CFD) [34–37], have been proposed. In these methods, computer technology and numerical analysis tools are applied, proving their practical usability. However, with the incomplete knowledge about the abrasive-wear mechanism, it should be noted that application of even the most sophisticated research methods does not guarantee reliable estimation of the actual course of wear of the elements working in soil. This is especially true for elements characterized by complex geometrical structure, in which materials with various tribological properties are used. For such elements, field examinations must be conducted in order to verify the quality of the obtained material-design solutions and to provide information about their usability. It should be noted that it is still valid to search for constructional solutions of the elements working in soil that, at relatively low.

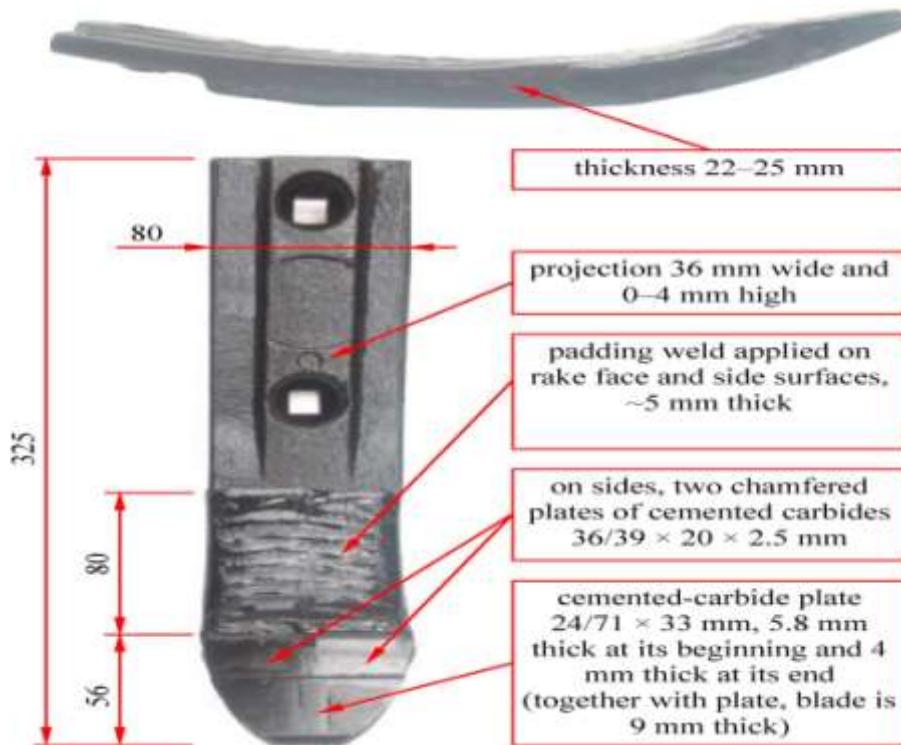


Fig. 1. Cultivator couler used in tests – variant A/1.

production costs, would be resistant to abrasive wear and the impact of stones in the soil. Certainly, a design solution of such elements includes their geometry and material composition. It seems that manufacturers of replaceable elements for equipment designed for work in soil or ground are aware of this and are aiming to develop cheap and durable elements. A known method for increasing the abrasive resistance of elements, which has been used in agricultural practice for many years, is the hardfacing technique. Practical experience in this field is supported by a series of investigations aimed at identifying the determinants of abrasive resistance of the padding welds. In this approach, laboratory tests were carried out in accordance with ASTM G-65, in which welding materials with different chemical compositions were evaluated [38,39]. The influence of the hardfacing process parameters and the microstructure on the abrasion resistance was also analysed [21,40]. In laboratory tests, cemented-carbide was also studied, which currently belongs to materials commonly used for reinforcing elements working in soil. The research aimed to determine the mechanisms of wear and the abrasive resistance of cemented-carbide depending on the size of the WC grains and the proportion of the matrix [41-44]. Our research is aimed at determining the wear resistance of selected cultivator coulters reinforced by hardfacing and brazing-on plates made of cemented carbides.

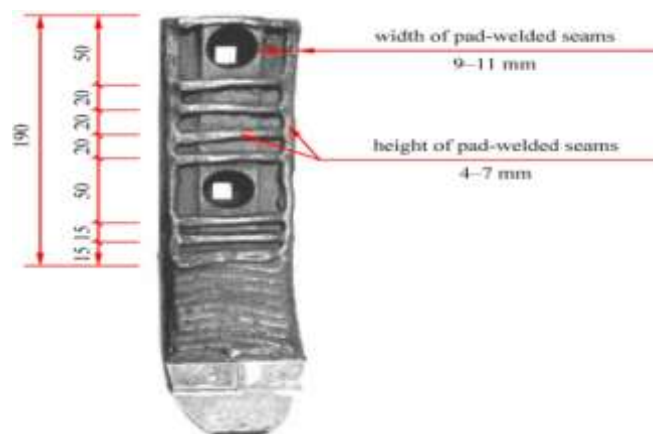


Fig. 2. Cultivator couler used in tests – variant A/2. Other dimensions are

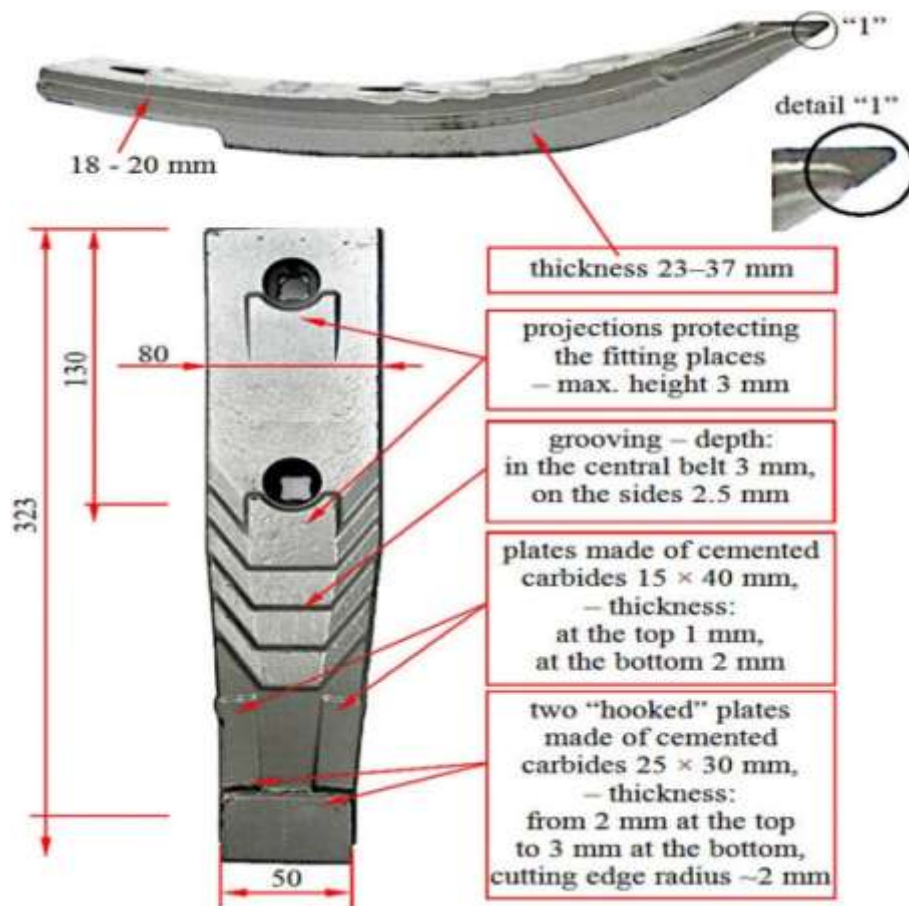


Fig. 3. Cultivator coulters used in tests – variant B.

MATERIALS AND METHODS

Figs. 13 show images with added basic information about the design of the cultivator coulters used in the research (marked with symbols A/1, A/2, and B). The A/1 and A/2 coulters were reinforced by the manufacturer with cemented-carbide plates and by hardfacing. The carbide plates were brazed on rake faces at the tip areas of the elements, and the pad-welded material was applied on the surface above the plates (Fig. 1). The A/2 coulters were additionally reinforced by pad-welding in the form of individual seams applied above the hardfaced area (Fig. 2). However, the B coulters (Fig. 3) were reinforced by the manufacturer with two plates made of cemented carbide shaped to protect the coulters blade (Fig. 3, detail "1") and with two more plates placed above them. Due to the curvature of the working surface of all types of tested coulters, the angle between this surface and the direction of movement gradually increased from the minimum value of about 35° (for the blade) to 60° (for the end area of the coulters). The A/2 and B coulters have not been the subject of research so far, here as the A/1 coulters have already been studied by the authors [27]. Previous research was conducted under different cultivation conditions than those in the present tests, so in the case of the A/1 coulters, the results of two tests under different working conditions could be compared. Due to comparable problems in both investigations, similar methods were used (chemical composition and hardness of materials, assessment of working conditions, and changes in geometry).

The chemical composition of individual materials used in the coulters was determined using a GDS 500AL glow discharge analyser and a JEOL JED-2300 energy-dispersed X-ray spectrometer (EDS, EDX) coupled with a JEOL JSM-6610A scanning microscope. SEM observations of the microstructures were carried out on the JEOL JSM-6610A scanning microscope, using topographic contrast (SE detector) and material contrast (BSE detector). Microscopic examinations were performed using a Nikon Eclipse MA200 light microscope with a Nikon DS-Fi5 CCD camera on etched specimens (the base material of coulters was etched with 3% HNO_3 ; pad-welded materials and carbide plates were etched electrolytically in H_2CrO_4). Vickers hardness was measured on a Zwick 321 tester at 9.807 and 294.2 N for 15s.

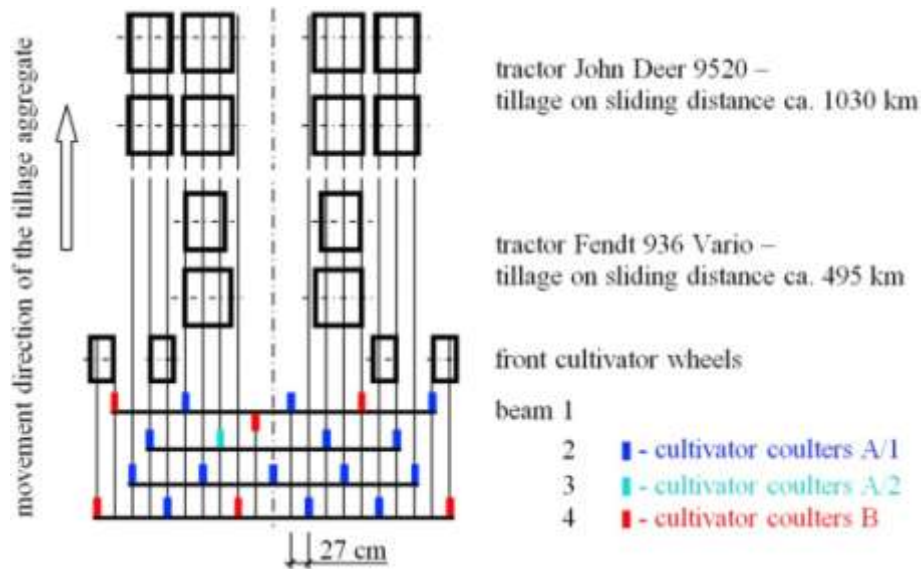


Fig. 4. Arrangement of examined coulters on cultivator beams.

Table 1 Working conditions of examined elements.

Quantity	Soil layer	Parameter value
Percentage of soil grade, %	arable	sandy loam (gl) -

soil grades present in the cultivated area were determined based on information from soil-agricultural maps covering the test area. These maps were developed some time ago, when the soil classification in Poland was somewhat different to the current classification. In Table 1,

layer

41

loamysand (pgm) -

26

(pgmp) -

next to the information on the percentage of individual soil grades, the symbols used in the former polish classification are given in brackets. These symbols are used in the description below. According to the data from the soil-agricultural maps, the cultivated soils were sandy loam (gl)

light loamy sand

12

(pgl) -

10

-41%), loamysand (pgm-26% and pgmp-12%) and light loamysand (pgl - 10% and pglp - 9%) (Table 1). According to the former classification-

Percentage of gravel (0.2-3 cm),

(pglp) 9

loam (gsp) 1

siltloam (plz) 1

cation, sandy loam (gl) contains 20%-35% of particles with $d < 0.02$ mm. Loamy sand (pgm) mainly contains particles with

$d \geq 0.1-1$ mm and 15%-20% of particles with $d < 0.02$ mm, and light

2.6 s $\frac{1}{4} 0.9$

%

loamy sand (pgl) mainly contains particles with $d \geq 0.1-1$ mm and 10%-

Percentage of fine stones (3–9 cm)

9.6 pc./m² s ¼ 4.0 pc./m²

0.50 kg/m² s ¼ 0.32 kg/m²

15% of particles with d < 0.02 mm. In addition, sands containing 25%– 40% of particles with d ¼ 0.02–0.1 mm are named silty soils (pgmp,

Percentage of humus, % 1.78 s ¼ 0.25

Reaction, pH_{KCl} 5.52–6.88

Actual humidity, wt% 0–10 cm 12.7 s ¼ 1.7

10–20 cm 12.2 s ¼ 1.6

Volumetric density, g/cm³ 1.33 s ¼ 0.09

pglp).

Standard results of the granulation measurements of the cultivated soils according to the currently used principles are presented in Table 2. According to the tillage technology used in the company where the

Soil compaction kPa Shearing stress, kPa

Working depth, cm Working speed, m · s^{–1}

s – standard deviation.

10–20 cm 1.52 s ¼ 0.07

0–10 cm 1231 s ¼ 621

10–20 cm 2141 s ¼ 828

0–10 cm 42 s ¼ 16

10–20 cm 62 s ¼ 22

10.6 s ¼ 2.0

2.88 s ¼ 0.24

tests were carried-out, the planned area was to be tilled twice with a cultivator. The depth of tillage was first ~10 cm and then ~20 cm. Basic examinations of the wear resistance of the coulters were carried out until the tillage was 10 cm deep. During this tillage, the sliding distance of the coulters was 1524.9 km, while the three coulters reached their wear limit at shorter sliding distances. After operation in soil, the coulters were examined with regard to changes in their geometry. Using the 3D Atos Triple Scan 3D GOM optical scanner, the change in the geometry of the coulters was evaluated through comparison with 3D models of new

In the tests, a 4-beam cultivator was equipped with 6 teeth on the first beam, 4 on the second, 5 on the third, and 6 on the fourth beam. In this investigation, 14 coulters marked with the symbol A/1, 1 coulters marked with A/2, and 6 coulters marked with B were installed as shown in Fig. 4. Because the distance between the traces of the teeth from the third and fourth beam was the same (27 cm) in relation to the traces of the teeth from the first and second beam (27 cm), the teeth from these beams worked under similar conditions (Fig. 4). Thus, the forces exerted by the soil on the teeth installed on the third and fourth beam were the same.

Tables 1 and 2 present the data on the working conditions of the examined coulters. Methods for measuring the value of the soil parameters were presented in the work by Stawicki et al. [27]. Percentages of coulters. Thus, the reduction in the length and the change in the width and thickness at the selected measurement points were established (Fig. 5). The obtained results of the geometry measurements allowed estimation of the intensity of linear wear at the selected measurement points. This intensity was calculated as the ratio between the material loss and the travelled sliding distance of the elements. It should be added that, in the A/1 and A/2 coulters, the carbide plates were brazed-on in such a way that the base material protruded beyond the plates (Fig. 1), on average 3.2 mm in the measurement line L2 (axis of the element). When determining the extent of length reduction of these coulters, this protrusion was taken into account. The sliding distance was determined using the working distance counter, which the cultivator was normally equipped with from its manufacturer (reading accuracy 0.01 km, in

Standard percentages of granulometric fractions in the cultivated soil (soil layer 0–10 cm).

No. sand	Percentage of granulometric fraction, %							Granulometric group		
	coarse			medium	fine		very fine	silt		clay
very coarse	coarse	medium	fine	very fine	coarse	fine	< d	d 0.002		
	1.0 < d 2.0	0.5 < d 1.0	0	0.25 < d 0.5	0.10	0.02	< d	0.05		

Testing the Wear of Cultivator Coulters in Forced with Cemented-Carbide Plates

0	5.6	$<d 0.25$ $0.05 < d < 0.10$			$0.002 < d < 0.02$		5.9	fsl
1	1.9	12.1	29.1	19.9	11.8	13.7		
2	2.3	7.0	13.8	26.7	17.0	10.7	16.6	5.9
3	2.1	5.0	11.1	25.1	15.5	12.7	22.6	5.9
4	2.1	6.7	17.7	35.2	18.6	7.9	7.9	3.9
5	1.7	6.0	14.7	31.1	19.0	12.8	10.8	3.9
6	1.9	5.8	13.7	24.8	23.4	10.8	13.7	5.9
7	1.7	5.4	14.0	26.2	17.3	12.8	17.7	4.9

d – size of soil grains, mm; fsl – fine sandy loam, lfs – loamy fine sand.

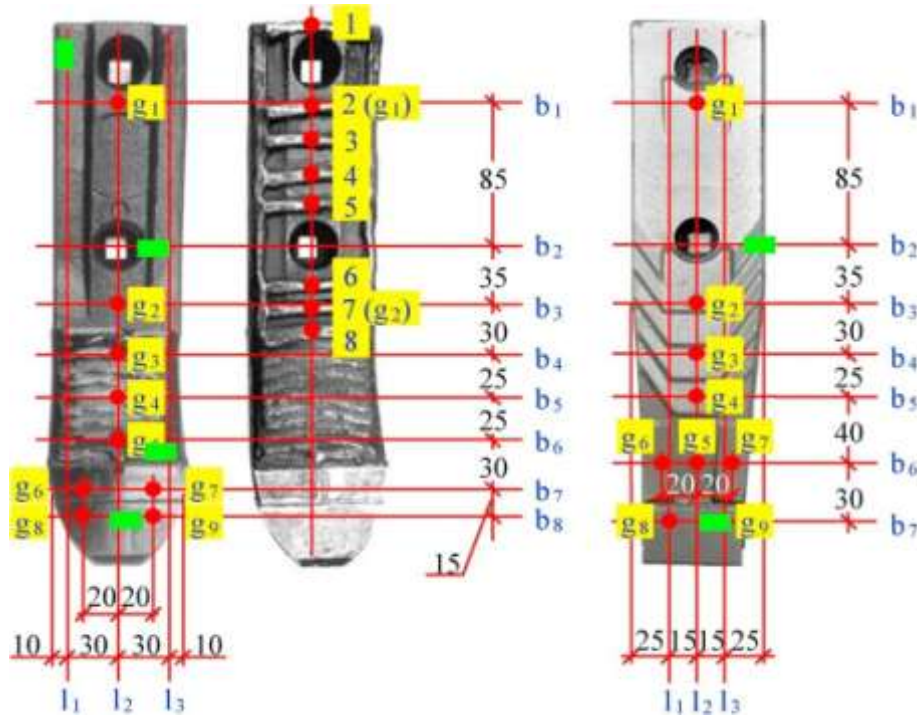


Fig. 5. A/1, A/2, and B coulters – measurement points of geometry

changes: l_1, l_2, l_3 – length measurement points, $b_1, b_2, b_3, b_4, b_5, b_6, b_7, b_8$ – width measurement points; $g_1, g_2, g_3, g_4, g_5, g_6, g_7, g_8, g_9$ (for the A/2 coulters in addition: 1, 2, 3, 4, 5, 6, 7, 8) – thickness measurement points; lines of cross-section measurements: elements A/1 and A/2: $l_1, l_2, l_3, b_1, b_2, b_3, b_4, b_5, b_6, b_7, b_8$; element B: $l_1, l_2, l_3, b_1, b_2, b_3, b_4, b_5, b_6, b_7$; areas of surface roughness measurements: element A/1, A/2 and B: places g_1, g_2, g_4 and between $g_8 - g_9$.

Table 3

Chemical composition and hardness of materials used for the A/1, A/2, and B coulters.

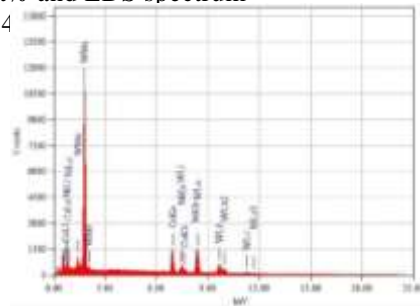
Material	Designation	Value A/1 and A/2 coulters
Base material	Chemical composition wt%	C 0.328; Mn 1.300; Si 0.272; P 0.027; S 0.014; Cr 0.342; Ni 0.062; Mo 0.013; V 0.002; Cu 0.274; Al 0.026; Ti 0.042; Co 0.009; B 0.003; Pb 0.005; Zr 0.013; rem. Fe

Plates of cemented carbides

Hardness, HV1 433 \pm 49

Chemical composition wt% and EDS spectrum

WC 79.79; Co 15.67; Ni 4



Surface padding weld

Padding weld in form of seams, (coulters) A/2

B coulters

Hardness, HV30 986 \pm 47

Chemical composition wt% C4.320; Mn0.373; Si1.040; P0.005; S0.015; Cr16.790;

V 0.039; Cu 0.080; Al 0.189; Ti 0.078; Nb 3.920;

Co 0.084; W 0.037; N 0.031; rem. Fe

Chemical composition wt% C3.670; Mn0.438; Si0.881; P0.005; S0.012; Cr14.160;

V 0.029; Cu 0.104; Al 0.191; Ti 0.071; Nb 3.350;

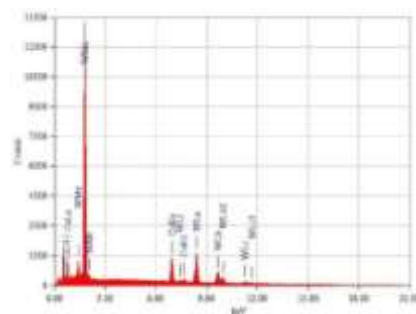
Co 0.070; W 0.028; N 0.041; rem. Fe

Base material Chemical composition wt% C0.392; Mn1.450; Si0.307; P0.011; S0.022; Cr0.448;

Ni 0.106; Mo 0.044; V 0.002; Cu 0.158; Al 0.036;

Ti 0.034; Co 0.009; B 0.002; Pb 0.005; Zr 0.013 rem. Fe

Plates of cemented carbides



Hardness, HV1 531 \pm 49

Chemical composition wt% and EDS spectrum

WC 85.65; Co 14.35

s – standard deviation.

Hardness, HV30 1057 \pm 457

manganese sulphides (Fig. 6). The presence of ferrite and manganese sulphides in the structure could decrease the abrasive-wear resistance of these steels. The hardness of the steel used in the B coulters was approximately 1.2 times higher than that used in the A/1 and A/2 coulters.

The cemented-carbide plates used in the A/1 and A/2 coulters were characterised by more fine-grained structure and slightly lower hardness in comparison to the plates used in the B coulters (Fig. 6 and Table 3). The grain size of tungsten carbide was determined in accordance with the PN-EN ISO 4499-2:2008 standard. The cemented-carbide grain size was classified as fine (about 0.8–1.3 μ m) for the A/1 and A/2 coulters and as coarse (2.5–6.0 μ m) for the B coulters.

Figs. 7a and 8 show the cross-sections of the padding welds used in

the A/1 and A/2 coulters, respectively, as well as the cross-section of the pad-welded seams additionally used in the A/2 coulters, together with hardness measurements taken every 0.5 mm (first measurement was taken approximately 0.2 mm from the pad-welded face). The difference between the maximum and minimum hardness of the pad-weld was 120.3 HV1 (Fig. 7a), and the difference in the hardness of the pad-welded seams was 300.4 HV1 (Fig. 8a). The pad-welded material was characterised by a heterogeneous macrostructure and microstructure. Fig. 7b shows the microstructure of the padding weld used in the A/1 and A/2 coulters, consisting of three layers. In the subsurface layer, large primary chromium carbides were identified in the matrix of a mixture of austenite and chromium carbides, most often characterised by lath structure and irregular distribution. Locally, the occurrence of niobium carbides was identified (Fig. 7b-1 and 1a). The subsurface layer progressively changed to the next layer with the highest hardness, which was composed of a more dispersive matrix including primary chromium and niobium carbides (Figs. 7b-2 and 2a). The number of primary chromium carbides decreased with the distance from the face of the padding weld. The lowest layer, located close to the fusion line, showed dendritic structure of austenite. Fine carbides and austenite were relocated in the interdendritic areas. In these areas, no primary chromium carbides were identified and the quantity of fine-dispersive niobium carbides was small (Fig. 7b-3 and 3a).

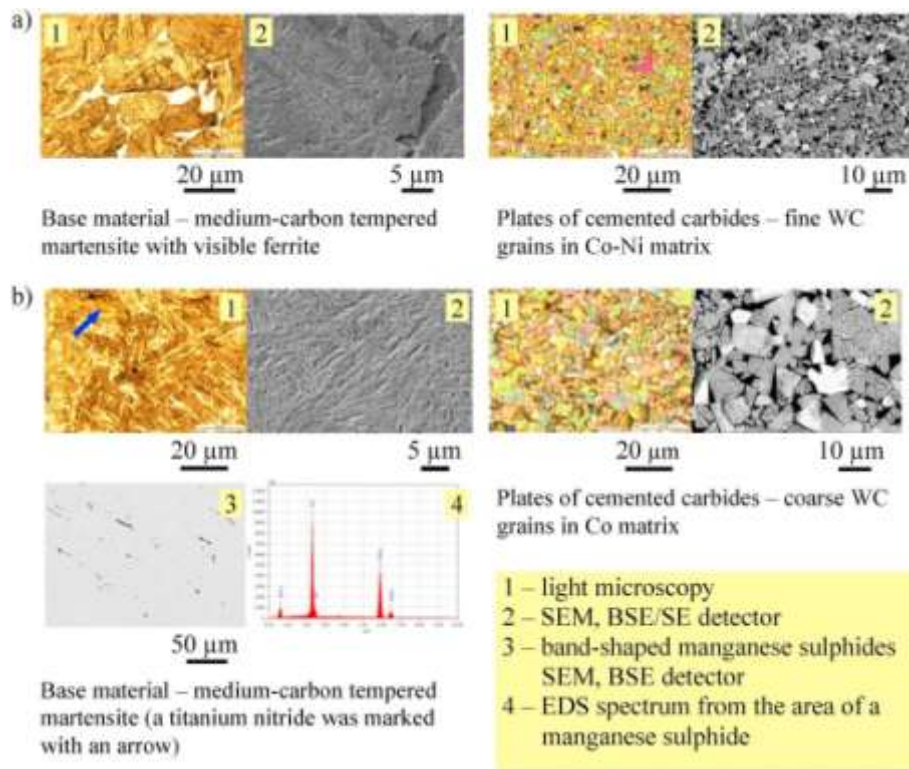


Fig. 6. Microstructure of base material and plates made of cemented carbide: a - A/1 and A/2 coulters, b - B coulters.

In the padding weld applied on the A/2 coulters in form of individual seams, two layers with highly different hardness were found (Fig. 8a). In the surface layer, the presence of large primary chromium carbides in the matrix of austenite and fine chromium carbides was found. Much more dispersive niobium carbides were also observed (Fig. 8b-1 and 1a). The lower layer of the padding weld, characterised by much lower hardness, was built of dendritic austenite and eutectic mixture in the interdendritic areas. The presence of a large quantity of evenly distributed fine niobium carbides was also found (Fig. 8b-2 and 2a).

It can be supposed that the differences between structures of both padding welds were related to the action of heat supplied at applying individual layers, which resulted in different hardness and microstructure of the welded material.

The brazing alloys used for fitting the carbide plates to the coulters varied with respect to their chemical compositions, but they were all typical alloys used for this purpose. The Cu48ZnNi10 brazing alloy was identified for the A/1 and A/2 coulters and the Cu67MnNi9 brazing alloy for the B coulters.

3.2. Description of the wear of the coulters

When evaluating the general geometry changes of the coulters, it should be noted that the average depth of their operation in soil was 10.6 cm. Due to shapes of the elements and their setting angle in the cultivator, the coulters were plunged in soil approximately to a half of their length during operation. As a result of dynamic action of inertial forces, the soil moved on the coulters surface above their penetration depth.

Fig. 9 show the stages of wear of the A/1 and B coulters. In both cases, the geometry change consisted mostly of length reduction. The thickness of the coulters was also reduced, especially in the area beyond the padding weld for the elements A/1 (Fig. 9a) and beyond the carbide plates for the elements B (Fig. 9b). It was characteristic in the B coulters that, as a result of the abrasive action of soil, a groove was created between the side carbide plates, running along almost the entire length of the elements (Fig. 9b). A reduction in the width was also observed in the top area of these coulters.

With the above-described form of wear, the wear limit of the coulters was determined by their length reduction of the bearing part that were exposed to abrasion. In the case of two A/1 coulters, emergency wear occurred, i.e. they were broken during lowering from the transport position to the working position. The fracture was characteristically located in the cross-section where the coulters were weakened by holes for assembly bolts and, in addition, by a relatively large reduction of width (Fig. 9a) and thickness (Fig. 10) in that area. As a result, during further operation, the weakened fittings of the coulters could be broken off in the case of an overload caused by hitting stones present in soil. However, the B coulters did not undergo any emergency forms of wear. Fig. 10 shows the A/2 coulters whose wear limit condition was also related to the reduction of length. The hard facing used in the form of pad-welded seams significantly contributed to less intensive material loss in the upper zone of the rake face (above the lower assembly hole). In practice, thickness reduction did not occur in this zone of the A/2 coulters (Fig. 10) since, during operation, soil was retained in the areas between the pad-welded seams, protecting the base material against wear, and only the harder padding weld material was subjected to abrasion (Fig. 11). It should be added that for working elements operating in soil, replacement of the "metal-soil" friction type with "soil-soil" friction may be unfavorable in terms of energy consumption of cultivation, due to the higher friction resistance of "soil-soil" friction type. However, the pad-welded seams below the lower assembly hole were completely rubbed-off (Fig. 11) and the base material in this area was subjected to wear, although to a lesser degree than it was in the A/1 coulters (Fig. 10). The boundary between the retained fragment of the pad-welded seam and the abraded zone coincided with the boundary of penetration in soil.

Fig. 12 illustrates the two quite typical observed phenomena related to wear of the coulters, i.e. spalling of the cemented-carbide plates and

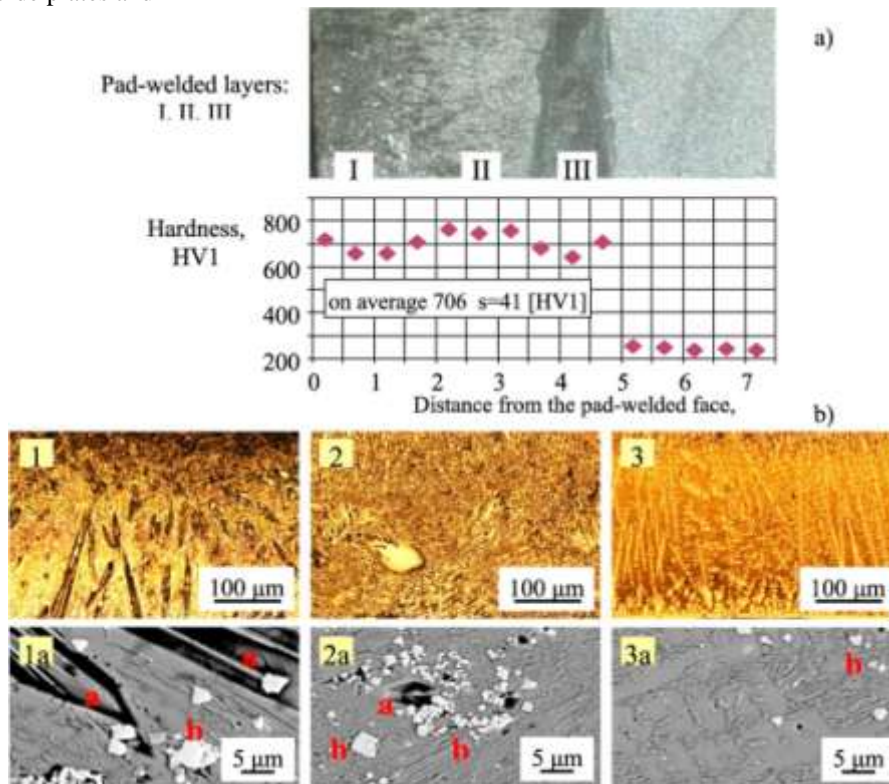


Fig. 7. Hardfacing weld (A/1 and A/2 coulters): a) macroscopic view and hardness profile;

b) microstructures of the weld layers: 1 and 1a–

irregularly arranged large primary chromium carbides (marked "a") in the matrix of a mixture of austenite with carbides, visible niobium carbides (marked "b"); 2 and 2a – fine-dispersive mixture of austenite and chromium carbides (marked "a"), visible fine niobium carbides; 3 and 3a – dendritic areas of austenite, fine carbides and austenite in interdendritic areas, locally visible niobium carbides (marked "b"). 1, 2, 3 – light microscopy; 1a, 2a, 3a – SEM, BSE detector.

washing-out of the welded material.

The spalling mechanism of the carbide plates is rather obvious. As a brittle material, carbides were subjected to spalling when hit by stones present in soil). However, the washing-out mechanism of the pad-welded material is not so obvious. It can be supposed that the washing-out mechanism occurred as a result of intensive abrasion of more soft base material of the coulter in front of the pad-welded area, which resulted in exposition of the weld face. As a result, the uncovered padding weld was more exposed to abrasive action of soil.

3.3. Intensity of the wear of the coulter

Fig. 13 shows the values of unit mass wear of the coulters. These values depended on the mass intensity of wear of the individual materials used in construction of the coulters. For the A/1 coulters fitted on the first and second cultivator beams, the values of this parameter were higher than those established for the elements from the third and the fourth beams – on average approximately 1.3 times. For the B coulters, the mass intensity of wear of the elements installed on the first cultivator beam was higher than that for the elements installed on the fourth beam – by approximately 1.7 times. Therefore, measurements of the unit mass wear of the coulters indicate more intensive wear of the elements

working with larger distances between the traces of operation of the teeth, i.e. the coulters installed on the first and the second beams of the cultivator. The A/2 coulter showed the lowest intensity of mass wear, which proves the effectiveness of the applied padding weld in the form of seams.

The unit reduction of the length, thickness and width of the examined coulters, obtained from the experiments, are shown in Figs. 14–16, respectively. Owing to the similar rate of wear of the A/1 coulters installed on the third and fourth beams, the results for these elements are combined in the figures. In some cases, the elements became worn in the planned measurement areas. Thus, several repetitions were carried out for the determined measurement areas. Therefore, in order to describe the variability of these parameters, standard deviations and ranges were used, as far as possible. In some measurement areas, the parameter value was not determined because of too aggressive wear (such areas are marked with an asterisk in Figs. 15 and 16).

For the A/1 coulters installed on the first cultivator beam, the intensity of length reduction at the measurement line L_2 (coulter axis) was 2.4 times higher than that for the elements installed on the second beam and 3.6 times higher than that for the elements installed on the third and fourth beams (Fig. 14). However, for the B coulters, the value of this parameter for the elements installed on the first beam was 8.3 times

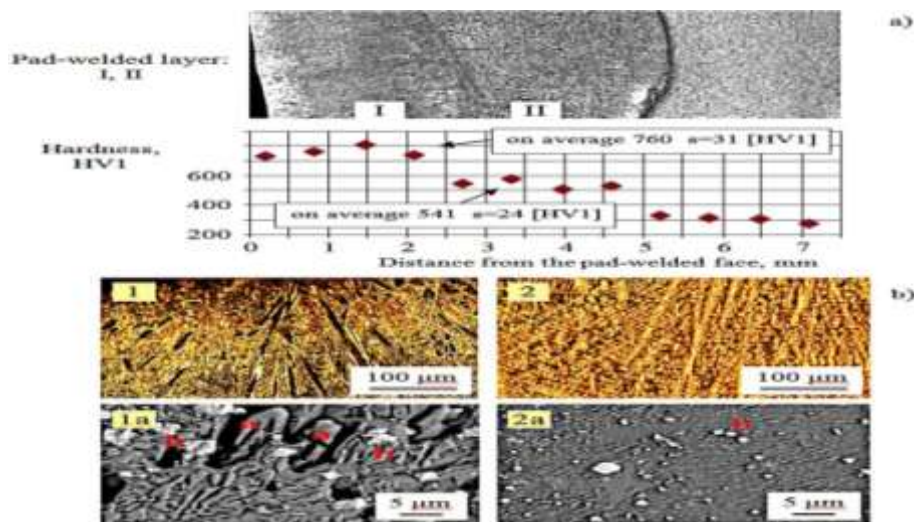


Fig. 8. Hardfacing weld in the form of a seam (A/2 coulter): a) macro

scopic view and hardness profile; b) microstructures of the weld layers: 1 and 1a – irregularly arranged large primary chromium carbides (marked "a") in the matrix of a mixture of austenite with carbides, visible fine niobium carbides (marked "b"); 2 and 2a – dendritic areas of austenite, fine carbides and austenite in interdendritic areas, visible fine, evenly distributed niobium carbides (marked "b"). 1, 2 – light microscopy; 1a, 2a – SEM, BSE detector.

higher than that for the elements installed on the fourth beam. This indicates distinctly harder working conditions for the elements on the first beam, which interact with soil having an untouched structure, thus lowering the load exerted to the soil by the coulters on the subsequent cultivator beams.

It was observed during the tests, that length reduction of the coulters installed on the first cultivator beam is irregular. This was reflected by the high values of standard deviation of the parameter of unit length reduction of the A/1 and B coulters. Such course of wear was caused by the spalling of the cemented-carbide plates when they hit against stones randomly distributed in the soil. According to the authors, the coulters installed on the first beam were particularly exposed to that wear mechanism, when they hit against stones present in soil. However, this facilitated shifting of the stones by the coulters installed on the subsequent cultivator beams, since the soil was already partially hoed by the elements operating before. Due to the described phenomenon, higher wear intensity of the coulters working in the track of the tractor wheels, thus cultivating the possibly more compressed soil, was not found.

No significant differences were found between the length reduction rates of the A/1 and A/2 coulters installed on these cond beam of the cultivator. However, unit length reduction values for the B coulters

installed on the first beam were on average 1.7 times higher than those for the A/1 coulters installed on the same beam (on the basis of the parameter values in the L_1 , L_2 and L_3 lines). The unit length reduction values for the B coulters installed on the fourth beam and for the A/1

coulters installed on the third and fourth beams were comparable – on

average 7.9 and 9.3 mm/10³ km, respectively for the B and A/1 coulters. The highest unit thickness reduction of the A/1 coulters occurred at the measurement points g_1 , g_2 , and g_5 , see Fig. 15. The points g_1 and g_2 were located within the base material (point g_1 above the line of penetration into the soil), and the point g_5 was located in the area of the padding weld (Fig. 5).

An increased rate of wear at the point g_5 , which especially affected the A/1 coulters working on the first and second cultivator beams, can be related to heavy loading by the soil, resulting in complete wear-out of the pad-welded material, followed by abrasion of the base material with much lower hardness. In that area, the phenomenon of "washing-out" of the pad-welded material occurred, as shown in Fig. 12. A lower rate of thickness reduction of the coulters was observed at the measurement points g_3 and g_4 , owing to the protective action of the applied padding weld.

The cemented-carbide plates brazed on the A/1 coulters slowed



Fig. 9. Exemplary stages of wear of the coulters: a) A/1; b) B (1 - new element, 2 - elements after operation in soil).

down the thickness reduction of the elements to a higher degree than the pad-welded material (Fig. 15). Unit thickness reduction of the lower plate was larger (Fig. 15, measurement points g_8 and g_9) than that of the plates brazed-on behind (Fig. 15, measurement points g_6 and g_7) – approximately 1.4 times for the coulters on the first beam and 1.3 times for the coulters on the other beams.

The unit thickness reduction in the base material areas of the A/1 coulters (measurement points g_1 and g_2) was approximately 2.1 times higher than the reduction in the pad-welded area (measurement points g_3 and g_4 ; the point g_5 is not considered) and approximately 5.6 times higher than the area with the brazed-on carbide plates (measurement points $g_6, g_7, g_8,$ and g_9). The unit thickness reduction in the pad-welded area (measurement points g_3 and g_4) was approximately 2.6 times higher than that in the area with the brazed-on carbide plates (measurement points $g_6, g_7, g_8,$ and g_9). The above calculations were performed in consideration of the parameter values for the coulters installed on all the cultivator beams. It should be noted that the presented relations indirectly characterise the abrasion resistance of the analysed materials, since the surface loads of the coulters by the soil were different at individual measurement points (the soil pressure systematically increased towards the blades of the elements).

The padding weld in form of seams used in the A/2 coulters significantly lowered the amount of thickness reduction of these elements compared to the A/1 coulters installed on the second beam of the cultivator (Fig. 15). At the measurement point g_1 , the amount of thickness reduction of the A/1 coulters was approximately 6.9 times higher than that for the A/2 coulters (measurement point g_1 was located in the zones of the A/1 and A/2 coulters that were not plunged in soil). At the measurement points 6, 7 (g_2) and 8, located in the penetration area of the A/2 coulters, the material of the pad-welded seams was completely worn (Fig. 11). Nevertheless, at the measurement point g_2 , the amount of thickness reduction of the A/1 coulters was about 1.3 times higher

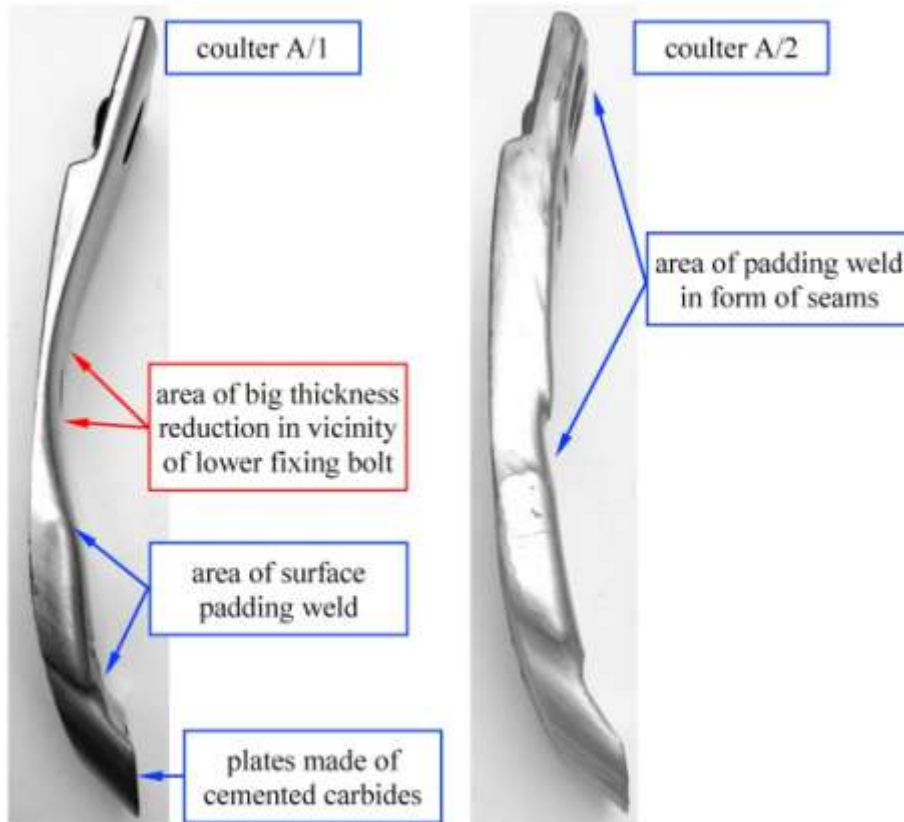


Fig. 10. Side view of the A/1 and A/2 coulters – clearly visible large thickness reduction of A/1 (sliding distance of both elements – 1524.9 km).

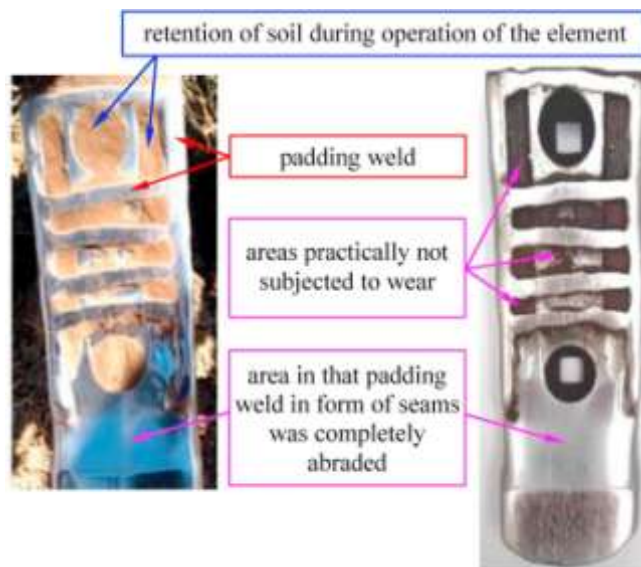


Fig. 11. Coulter A/2 – protective action of the padding weld in form of seams.

the working surfaces of the coulters. In contrast, a decrease in the parameter values at the measurement point g_5 most probably resulted from its location – between two carbide plates brazed on the sides of the coulters (Figs. 3 and 5).

Cemented-carbide plates relieved the base material, especially when a groove was formed between them as a result of the abrasive action of the soil (Fig. 9).

As was found for the A/1 coulters, the values of unit thickness reduction of the B coulters, measured in the areas of carbide plates (measurement points $g_6, g_7, g_8,$ and g_9), were lower than those for the base material. The ratio of the average unit thickness reduction of the coulters in the base material area (measurement points $g_1, g_2, g_3, g_4,$ and g_5) and the unit thickness reduction of the carbide plates (measurement points $g_6, g_7, g_8,$ and g_9) was about 8.7. Similarly, in the case of the B coulters, the values of unit thickness reduction of the lower plates were higher than those for the upper plates, by about 1.7 times (based on the wear of the plates from the coulters installed on the fourth cultivator beam).

It should be added that the estimated amount of thickness reduction of the cemented-carbide plates installed on the examined coulters were similar, which indicates similar abrasion resistance of the plates.

At all the measurement points, the lowest value of unit thickness reduction was that for the A/2 coulters. Therefore, the padding weld in the form of seams in this area also contributed to limitation of the abrasion intensity of the element, but to a lesser degree than it did in the area above, see Fig. 10. In the B coulters, the values of unit thickness reduction were also the highest for the base material area (Fig. 15). At the measurement points $g_1, g_2, g_3,$ and g_4 , the values of this parameter gradually increased, which corresponded with the increased pressure exerted by the soil on reduction was observed for the coulters installed on the third and fourth cultivator beams. As in the case of the B coulters, the values of unit thickness reduction were lower for the elements installed on the fourth beam (Fig. 15). Therefore, it can be stated again that the coulters installed on the back cultivator beams operate under less difficult conditions. A significant increase in the rate of width reduction of the A/1 and A/2 coulters was found in the measurement lines $b_6, b_7,$ and b_8 , located in the lower coulters areas (zone of padding weld and brazing of plates made of cemented carbides) (Fig. 16). However, in the B coulters, the highest rate of width reduction occurred in the measurement line b_5 , located in the area of the base material, above the cemented-carbide

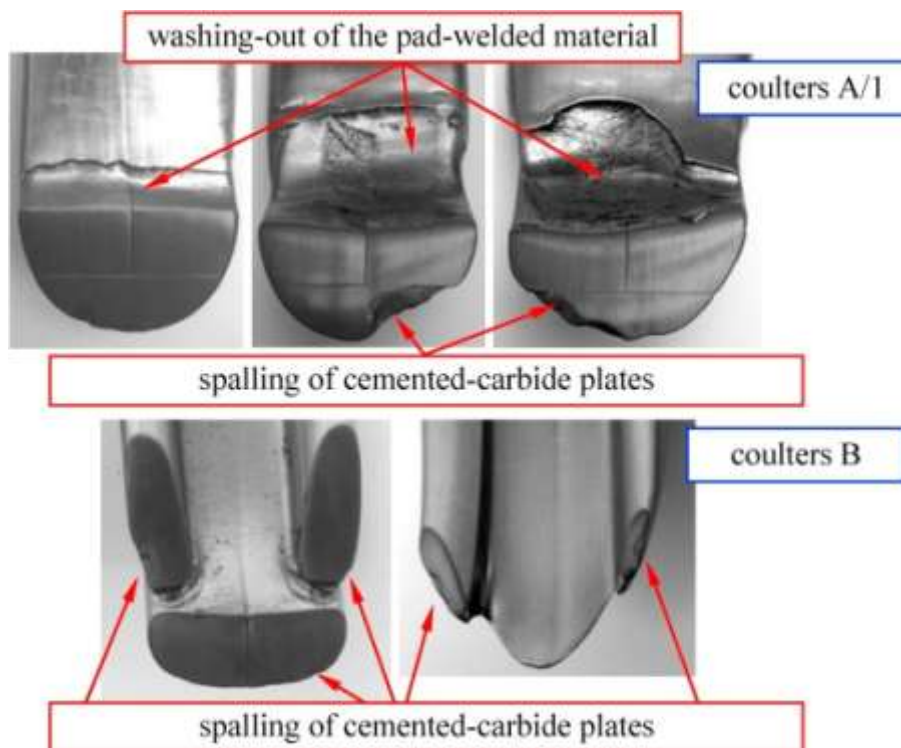


Fig. 12. Wear of top area of the A/1 and B coulters.

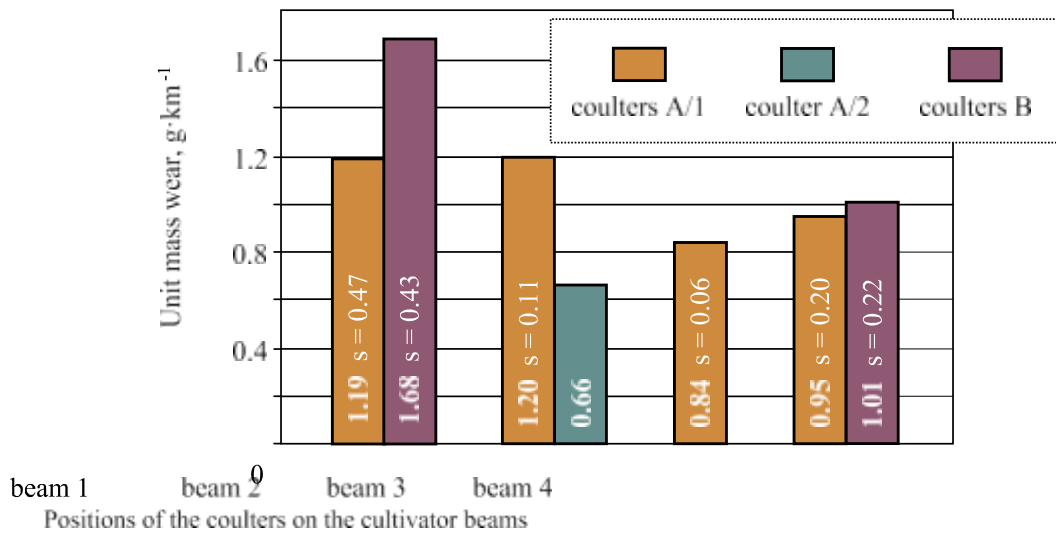


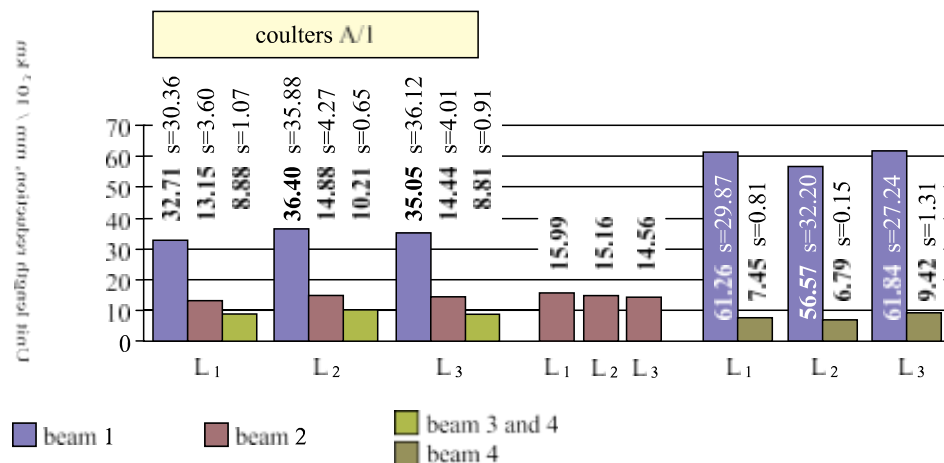
Fig. 13. Unit mass wear of the coulters (s – standard deviation).

plates (Fig. 16). Measurements of the unit width reduction of the A/1 and B coulters also indicate more difficult working conditions of the elements installed on the first cultivator beams compared to those installed on the subsequent beams. In the case of the A/1 coulters, this is especially visible in the measurement lines b₅, b₆, b₇, and b₈, but for the B coulters, this is observed in the measurement lines b₄, b₅, and b₆ (Fig. 16).

3.4. Mechanism of wear of the materials used in the coulters

In all the examined coulters, the wear process of the cemented-carbide plates proceeded in a similar way (Figs. 17 and 22). At the beginning, the matrix was abraded under action of the finest fractions of the abrasive mass. As a result, cracks and mass losses occurred around the carbide grains, weakening their mounting in the material. In the second stage of destruction, the weakened carbides were chipped-out from the matrix, which resulted in formation of characteristic craters owing to the removed carbide grains (pits) (Figs. 17 and 22). It was also found that a part of the carbides firmly seated in the matrix were subjected to crushing or cracking (Figs. 17b and 22b). In the A/1 coulters, in the initial area of partially worn carbide plates, i.e. in the area most strongly loaded by soil, grinding effects were identified with cracks covering many carbide grains and propagating deep into the plates (Fig. 17a). A similar effect, although less intensive, occurred in the B coulters (Fig. 22b).

The condition of the surfaces of the padding welds used in the A/1



Measuring place (Fig. 5)

Fig. 14. Unit length reduction of the coulters (s – standard deviation).

and A/2 coulters after their application in soil is shown in Figs. 19 and 21. The padding welds were characterised by the presence of cracks that occurred during the hard facing process (Figs. 19c, 20 and 21a). In both the forms of padding welds, there were clear scratches in the movement direction of the soil particles. Wide and shallow grooving characterised by very small (Fig. 19) or even missing plastic deformation (Fig. 20) also occurred. The large primary chromium carbides characterised by high hardness and brittleness, present in the padding weld, contribute to the

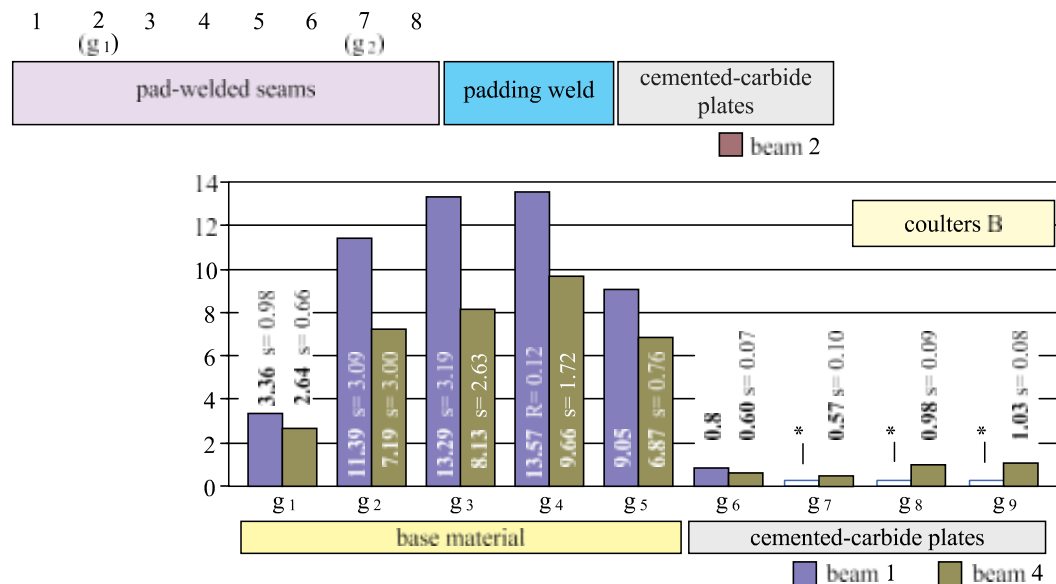
delamination of the material (Figs. 19c, 20b and 21). There were also areas where soil particles shifting over the weld surface removed the material around the firmly seated carbides (Fig. 19a). With regard to diversified, heterogeneous microstructure of the padding welds built of several layers, the effect of a complex process of abrasive wear was found. However, the dominating mechanism of wear was microcutting. In both steels used as base materials of the coulters, the dominant mechanism of wear was grooving and microcutting (Figs. 18 and 23). The observed scratches related to the microcutting mechanism were characterised by small width and larger depth in comparison to the grooves (Figs. 18a and 23a). In general, the direction of grooves and scratches coincided with the movement direction of the abrasive fraction; only a small part was distinguished by other directions. More plastically deformed areas were found on the surfaces of the A/1 coulters, which can be explained by the higher plasticity of the base steel used in these coulters compared to the base steel used in the B coulters. Moreover, a ploughing effect was identified in the A/1 coulters, directed perpendicular to the movement direction of the abrasive fraction (Fig. 18c). On the surfaces of both examined steels, pinholes were also found (Figs. 18b and 23a).

The roughness measurement results of the rake faces surfaces of the coulters are represented in Table 4. Because of similar roug

ness values for the A/1 coulters on the first and the second cultivator beams and for those installed on the third and fourth beams, the average roughness values for all the A/1 elements installed on these beams are given. For the B coulters, it was impossible to measure the roughness at several measurement points because of the geometry of the elements after operation in soil (Fig. 9) and the limitations of the profilographometric method. Surface roughness (Ra) of the cemented carbide plates brazed on the A/1, A/2, and B coulters was about 3.0–3.4 times higher than that for the base material (at measurement points $g_8, g_9,$ and g_2). Similarly, the surface roughness (Ra) of the padding welds applied on the A/1 coulters on the first and second beams and the third and fourth beams was about 3.7 and 2.6 times higher than that for the base material times (at measurement points g_4 and g_2). The surface roughness (Ra) of the cemented carbide plates brazed on the B coulters was about 1.6 times higher than that of the plates installed on the A/1 and A/2 coulters. The statistical significance test showed that the average values of the parameters Ra, Rt, Rp, and Rv for the B coulters installed on the fourth beam are significantly higher than the values for the A/1 coulters installed on the third and fourth beams. This can be explained by the more coarse-grained structure of the carbide plates used on the B coulters and the wear mechanism dominated by crushing and chipping carbide grains from the matrix. In the case of the A/2 coulters, the measurements of the surface roughness of the padding weld in the form of seams (Fig. 5) were planned among others at the measurement point g_2 . During the operation, the weld material at this point was completely abraded, so the surface roughness measured at that point was related to the base material (this is why in Table 4, the material at g_2 is marked as “base”). The roughness of the pad-welded seam (measurement point g_1 situated above the zone of penetration in the soil) was slightly lower than that of the padding weld (measurement point g_4) (Table 4). This probably resulted from the fact that the surface of the welded seam was less loaded by soil, as well as from a slightly higher hardness of the material (Figs. 7 and 8). In the range of parameter Ra, it was found that the working surfaces of the pad-weld material and cemented-carbide plates have a higher roughness than the base material of the coulters, owing to the different wear mechanisms of these materials. This observation confirms the analysis of the relationship between the values of the parameters Rv to Rp. In general, for all the examined coulters, the ratio of the parameters Rv to Rp ranged between 1.3 and 4.0 for the base material, between ca. 1.8 and 3.9 for the padding weld in the A/1 and A/2 coulters, and about 1.5 for the welded seams in the A/2 coulters. In the case of the cemented-carbide plates, this ratio ranged from about 1.1 to 1.3. The surface condition of the base materials and the padding welds indicates a different course of destruction compared to the cemented carbide plates, for which the Rv to Rp ratio ranged from 1.1 to 1.3. The lower hardness of the base material and the padding weld corresponded with their higher susceptibility to destruction by elementary forms of abrasive wear, i.e. microcutting and scratching.

DISCUSSION

The results of mass wear and the results of wear intensity of the length, thickness and width indicate that the coulters installed on the first beam of the cultivator are under the hardest working conditions, owing to the impact of soil with an intact structure. In contrast, the



Measuring place (Fig. 5)

Fig. 15. Unit thickness reduction of the coulters (* – no data due to wearing of the elements at the measurement point, s – standard deviation, R – range).

intensity of wear of the coulters installed on the third and fourth beams was the smallest, indicating the lowest load of these elements in the soil. During operation of the examined coulters, their wear process was related to the reduction of length, thickness, and width. Figs. 24–26 show the longitudinal and perpendicular sections of the A/1, A/2, and B coulters. The presented conditions do not correspond to the limit wear condition of the coulters, but these figures show the proportions of material reduction along the elements and in the directions related to their thickness and width, as well as the places where the highest shape changes occurred. It can be seen in Fig. 24 that the thickness of the A/1 coulters was significantly reduced in vicinity of the lower assembly bolt (base material area) and its width was considerably reduced in its lower area (Fig. 24b, measurement points $b_6, b_7,$ and b_8). In previous research [38] where the A/1 coulters were used among others, more intensive thickness reduction was found in the base material area (unit thickness reduction at the measurement points g_1 and g_2 was about 1.1–2.6 times higher than the values found in our tests) and, at the same time, mostly less intensive thickness reduction of the padding weld material and the carbide plates was found. The unit length reduction of the A/1 coulters was also smaller (5.0, 3.5, and 1.5 times in the measurement line L_2 for the elements installed on the first, second, and third and fourth beams, respectively). Substantial thickness reduction resulted in breakages of the coulters, abrasion-through, or failure resulting from abrasion of conical heads of the assembly bolts. Such cases were not found in the present examinations (apart from the previously described breakage of two elements during lowering of the tool). The presented difference in the forms of wear of the A/1 coulters probably resulted from their different working conditions, in particular from the higher humidity of the cultivated soil (17.2%) (influencing its lower compactness – 691 kPa and lower shearing stress – 38 kPa) and

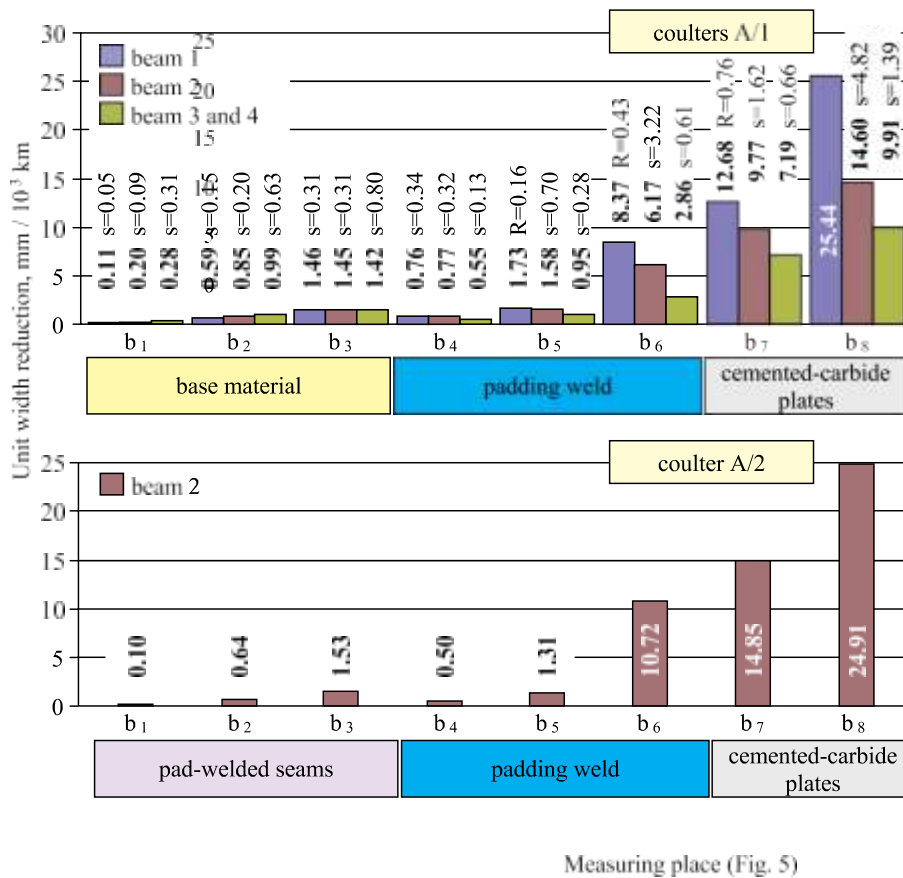


Fig. 16. Unit width reduction of the coulters (* – no data due to wearing of the elements at the measurement point, s – standard deviation, R – range).

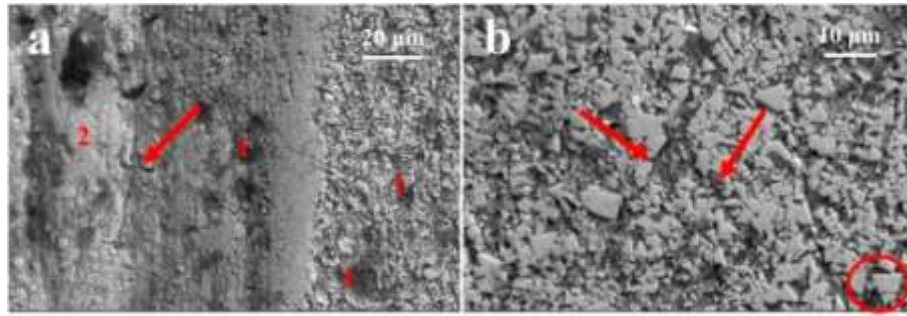


Fig.17. Worn surface of the fine grained cemented carbide plates in the A/1 coulters: a) pits (marked as "1"), area of extremely intensive grinding effect (marked as "2"), and a crack propagating inside the cemented carbide plate (marked with an arrow); b) fully cracked WC grains (marked with a circle) and cracks propagating inside the cemented carbide plate (marked with arrows). SEM, SE detector.

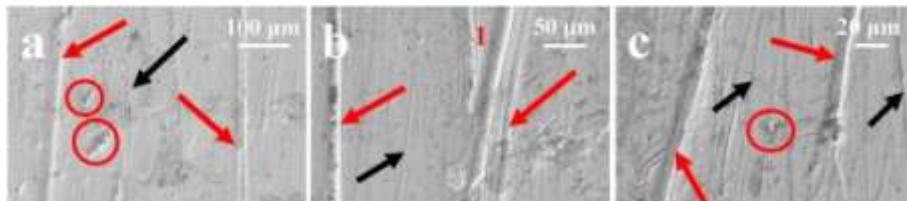


Fig. 18. Worn surfaces of the investigated steel used in the A/1 coulters: a) grooves (marked with red arrows), pinholes (marked with circles), scratches (marked with a black arrow), b) grooves (marked with a red arrow), scratches (marked with a black arrow) and plastically deformed material on a groove (marked as "1"), c) grooves (marked with a red arrow), scratches (marked with a black arrow), and ploughing (marked with a circle). SEM, SE detector. (For interpretation of the references to colour in this figure legend, the reader is referred to the Web version of this article.)

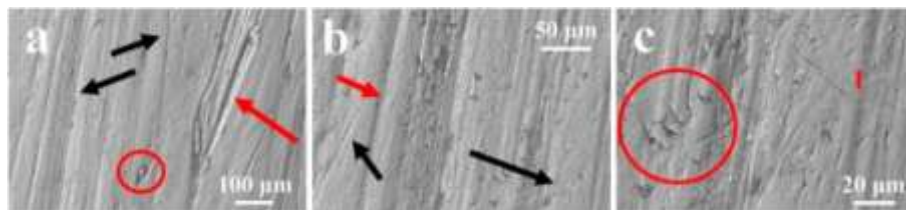


Fig. 19. Worn surfaces of the investigated padding weld used in the A/1 coulters: a) grooves (marked with a red arrow), scratches (marked with black arrows), and pressed-in particles (marked with a circle), b) grooves (marked with a red arrow), scratches (marked with black arrows), and pinholes, c) magnification of area shown in Fig. 4b, delamination (marked with a red circle), crack (marked as "1") and pinholes. SEM, SE detector. (For interpretation of the references to colour in this figure legend, the reader is referred to the Web version of this article.)

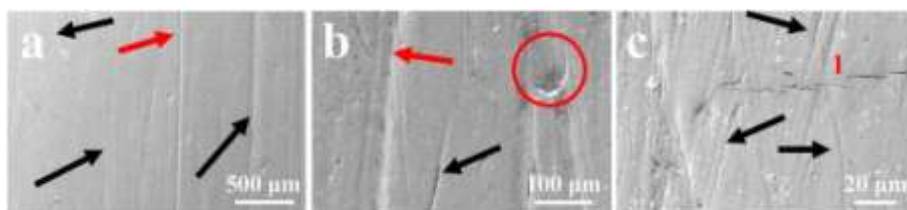


Fig. 20. Worn surfaces of the investigated padding weld used in the A/2 coulters: a) grooves (marked with red arrows), scratches (marked with black arrows), b) grooves (marked with red arrows), scratches (marked with black arrows), pinholes, and delamination (marked with circles), c) scratches (marked with black arrows).

black arrows), crack (marked as "1"), and a large number of pinholes. SEM, SE detector. (For interpretation of the reference to colour in this figure legend, the reader is referred to the Web version of this article.)

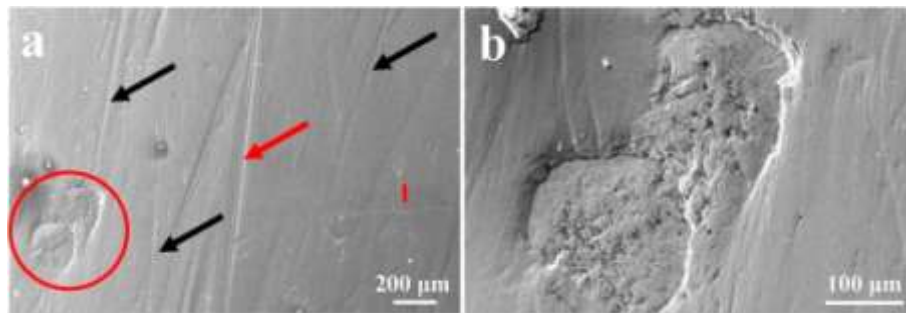


Fig.21.

Worn surfaces of the investigated padding weld used in the A/2 coulters: a) grooves (marked with a red arrow), scratches (marked with a black arrow), crack (marked as "1"), and delamination (marked with a circle), b) magnification of the delamination area shown in Fig. 6a, and visible pinholes. SEM, SE detector. (For interpretation of the reference to colour in this figure legend, the reader is referred to the Web version of this article.)

slightly deeper tillage (13.1 cm). In more humid soil, fastening of the abrasive grains (quartz) by its remaining fraction is weaker (this is indicated by lower compactness and lower shearing stresses occurring in humid soils). Thus, abrasive particles lose their wearing contact due to the lower forces acting on the abraded material, thus reducing their ability to wear the material. This can explain the less intensive wear of the cemented carbide plates and pad-welded material, as well as the less intensive length reduction of the A/1 coulters operating in more humid soil. In contrast, a larger unit thickness reduction of the coulters in the base material area (points g_1 and g_2) during operation in more humid soil can be attributed to the slightly larger depth of tillage and the higher plasticity of humid soil. Plastic soil can be more easily deformed and crushed, albeit to a lower degree. It can therefore be supposed that humid soil moved over the coulters surface in the form of a plastic monolith in permanent contact with the surface, as opposed to soil with lower humidity that is not subjected to crushing. Thus, permanent contact of humid soil with the coulters surfaces could result in more intensive thickness reduction at points g_1 and g_2 .

In contrast, the highest thickness reduction of the B coulters (Fig.26) occurred in the area between the carbide plates and the lower assembly

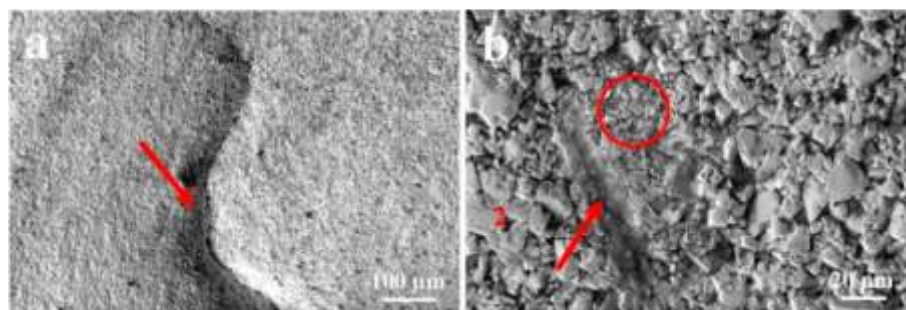


Fig. 22. Worn surface of the coarse-grained cemented carbide in the B coulters: a) pits on worn surface and visible crack propagating inside the cemented carbide plate (marked with an arrow); b) pits on the surface, grinding effects (marked with an arrow), and visible crushed (marked with a circle) and fully cracked (marked as "2") WC grains. SEM, SE detector.

bolt (base material area), and the highest width reduction occurred in the lower part of the element (Fig. 26b, measurement points b_5, b_6, b_7 – areas of the base material and the brazed-on carbide plates). In Fig. 26b, a groove is clearly visible in the coulters axis resulting from soil moving along the base material surface (measurement points b_3, b_4, b_5 , and b_6).

In summary, it can be said that the cemented-carbide plates used in the A/1, A/2, and B coulters were characterised by the highest abrasion resistance in relation to the other materials. Therefore, they effectively decreased the reduction rate of the thickness, length and width, while this limitation of length reduction is related to the stoniness of the cultivated soil because of the brittleness of the carbide plates. The padding weld used in the A/1 coulters also decreased the thickness reduction rate of the elements. In contrast, the pad-welded seams applied on the A/2 coulters additionally contributed to the limitation of the thickness reduction in the area above the padding weld, especially above the lower assembly bolt.

The coarse-grained and fine-grained carbide plates used in the examined coulters were subjected to similar mechanisms of wear: removal of the matrix under action of the finest fractions of the abrasive mass, next cracking, and crushing or chipping of carbides from the matrix. This was reflected by high values of roughness parameters of the plates surfaces. A similar wear process of carbide plates was found by Gee and others [45]. In our own research, cracks propagating inside the plates and covering a number of carbide grains were additionally observed. However, no subsurface cracks (parallel to the surface) were observed, similar to the findings of Gant and others [46].

During service of the coulters, crushing of the carbide plates occurred when they were hit by stones present in the soil. In the fine-grained carbide plates used in the A/1 and A/2 coulters, the percentage of the cobalt–nickel matrix amounted to about 20.2%, but in the coarse-grained carbide plates used in the B coulters, the percentage of the cobalt matrix amounted to approximately 14.3% (Table 3). Differences in the volume fraction of the matrix influenced the hardness, which was higher (1057 HV30) in case of the B coulters than the A/1 coulters (986

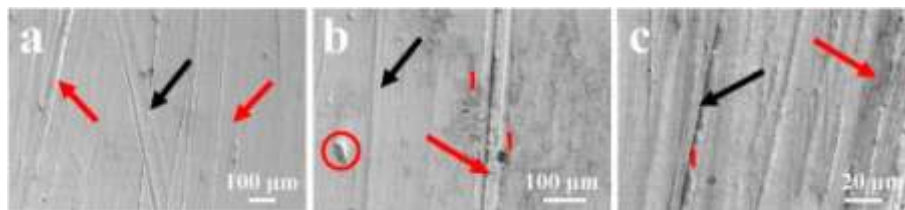


Fig. 23. Worn surfaces of the investigated steel used in the B coulters: a) grooves (marked with red arrows), scratches (marked with a black arrow) and pinholes, b) grooves (marked with red arrows), scratches (marked with a black arrow), large pinhole (marked with a circle), and plastically deformed material on a groove (marked as "1"), c) grooves (marked with red arrow), deep scratch with "extruded lip" (marked with a black arrow), plastically deformed material on a groove (marked as "1"). SEM, SE detector. (For interpretation of the reference to colour in this figure legend, the reader is referred to the Web version of this article.)

HV30). The proportion of the matrix and the grain size of the cemented-carbide materials determine their wear resistance [41–44]. However, the tested cemented-carbide plates revealed comparable wear intensity despite significant differences in the structure.

In order to increase the abrasive wear resistance of the A/1 and A/2 coulters, the hardfacing technique was applied, which is widely used in the mining, agriculture, and construction industries. The surface layer of the padding welds applied on the coulters was composed of large primary chromium carbides and relatively ductile eutectic mixture built of chromium carbides with austenite. In previous works [47–49], primary chromium carbides and carbides in the eutectic mixture, occurring in similar padding welds, were identified as carbides type M7C3. As was found in Ref. [50], large primary brittle chromium carbides, unevenly distributed in the weld structure, determine the irregular abrasive-wear processes and can result in delamination and crushing. Similar phenomena were observed in the present study. Below the surface layer, the fraction of dispersive niobium carbides in the welds increased (except the third, i.e. lowest, layer of the padding welds). It was demonstrated in Ref. [51] that the content of dispersive and evenly arranged niobium carbides significantly increase the abrasion-wear resistance and hardness of the welds. In summary, it can be said that the padding welds used in the A/1 and A/2 coulters, composed of two

or three layers with different structure and hardness, were subjected to unstable and uneven wear processes, which determined the rate of their wear.

The base materials of the coulters were martensitic steels with microadditives of boron, which increases the abrasive wear resistance of steel [16,17]. The surface roughness of the coulters in the base material area was low, so the wear process of that material was different than that of the carbide plates and padding welds. The dominant mechanism of wear of the base steels was grooving and microcutting with a relatively intensive course, as shown by the large thickness reduction of the coulters in the base material area in comparison to the areas of other materials characterised by higher hardness. It seems that a fine fraction of soils, whose particles are not so firmly fixed in the soil mass, was more significant in the wear of the base material than in wear of the other

Table 4
Roughness of rake surfaces of coulters after operation in soil.

Coulter and its fitting place		Measurement point (Fig. 5)	Roughness parameter value, μm				
			Ra	Rt	Rp	Rv	
A/1	Beam 1 and 2	g ₁ ¹⁾	0.40s=0.21	5.95 s=3.85	1.18 s=0.66	4.77s=3.22	
		g ₂	0.26s=0.03	4.21 s=1.40	1.40 s=1.18	2.81 s=0.81	
			0.96s=0.44	9.74s=3.76	2.84s=1.13	6.90s=2.67	
		g ₈	0.73 s=0.12	5.87 s=1.57	2.85 s=0.85	3.02s=0.75	
	Beam 3 and 4	g ₁ ¹⁾	0.42s=0.12	5.06 s=1.99	1.34 s=0.61	3.71 s=1.76	
		g ₂	0.20s=0.08	2.38s=0.98	1.02 s=0.76	1.36 s=0.49	
		g ₄	0.52s=0.18	7.12s=2.65	1.45 s=0.54	5.67 s=2.33	
		between and g ₉	0.77s=0.12	5.81 s=0.67	2.80s=0.47	3.01 s=0.71	
	A/2	Beam 2	g ₁ ¹⁾	0.89	7.30	2.91	4.39
			g ₂	0.24	2.35	1.23	1.12
			1.00	9.26	3.32	5.94	
g ₈			0.81	5.68	2.46	3.22	
B	Beam 1	g ₁ ¹⁾	0.36s=0.15	4.63 s=2.47	1.10 s=0.58	1.34 s=1.96	
		g ₂	0.38R=0.22	3.99R=2.15	1.09R=0.52	2.90R=1.33	
			*	*	*	*	
			**	**	**	**	

	g_8					
Beam 4	$g_1^{1)}$	0.50s=0.33	7.68 s=5.81	1.61 s=0.76	6.07	s=5.05
	g_2	0.37***	9.59***	2.48***	7.11***	*
	g_8	1.23 s=0.09	9.32s=0.32	4.05s=0.14	5.26	s=0.33

1) – measurement point situated above the zone of penetration in soil,
 * – no result due to wear geometry of the elements making the measurements impossible,
 *** – no result due to wear of the cemented carbide plates,
 – established for one element only due to wear geometry of the other elements making the measurements impossible
 s – standard deviation, R – range

materials. It should be added that the participation of grooving was the highest in the A/1 and A/2 coulters, which can be explained by the higher plasticity of the steel used in their structure, resulting from the presence of ferrite. In both types of the examined coulters, the directions of grooves and scratches were coincident with the movement direction of the abrasive mass. Only a small part had with different directions of grooves and scratches, which indicates that the abrasive fractions acting on the steel surface were diversified with regard to their grain coarseness.

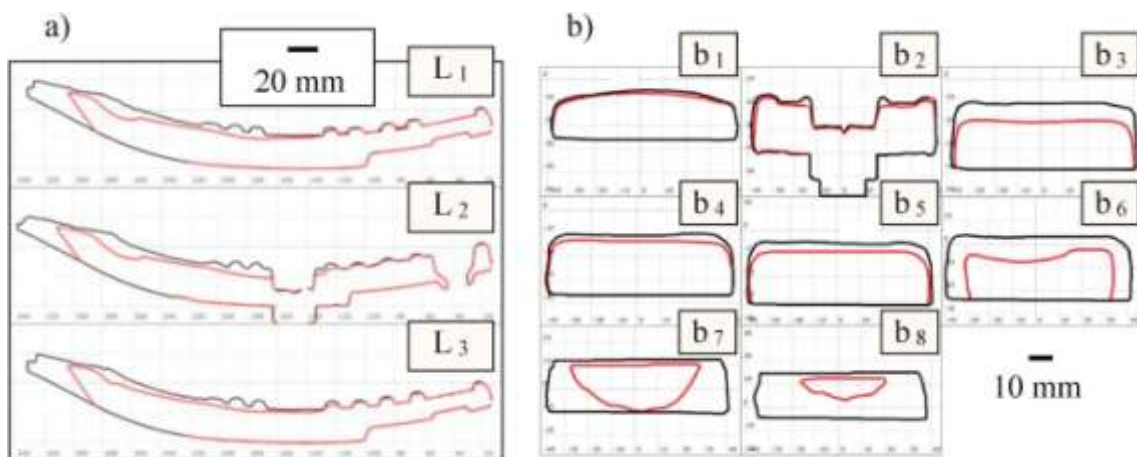


Fig.24. Cross-sections of the A/1 coulters (element installed on the fourth cultivator beam, sliding distance: 1524.9 km): a – longitudinal sections, b – perpendicular sections: b₁, b₂, b₃ – sections in the area of base material, b₄, b₅, b₆ – sections in the area of padding weld, b₇, b₈ – sections in the area of cemented carbide plates.

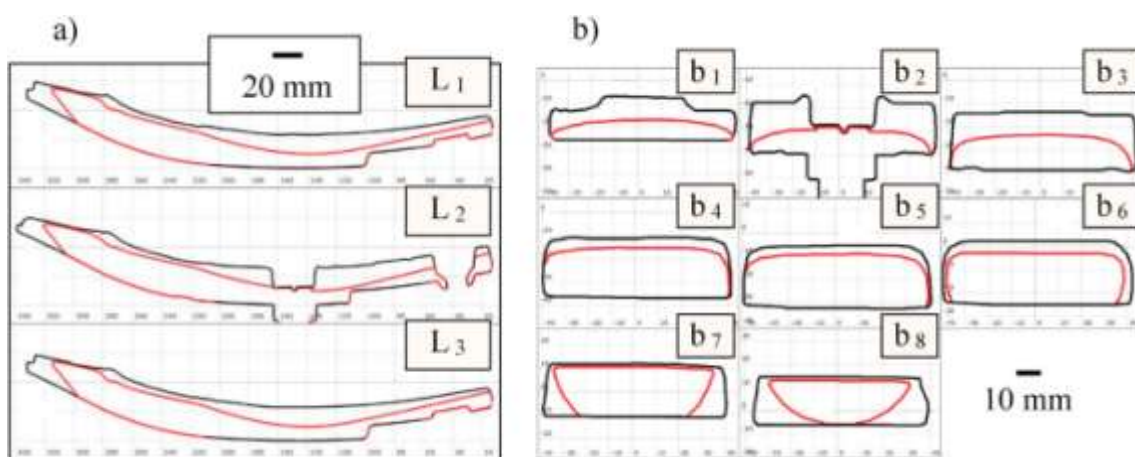


Fig. 25. Cross-sections of the A/2 coulters (element installed on the second cultivator beam, sliding distance: 1524.9 km): a – longitudinal sections, b – perpendicular sections: b₁, b₂, b₃ – sections in the area of base material, b₄, b₅, b₆ – sections in the area of padding weld, b₇, b₈ – sections in the area of cemented carbide plates.

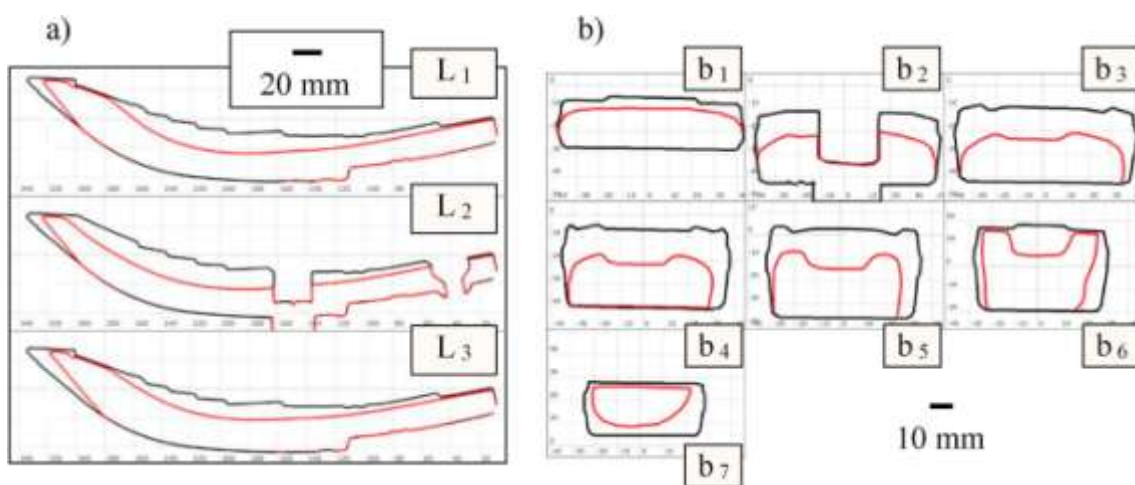


Fig. 26. Cross-sections of the B coulters (element installed on the fourth cultivator beam, sliding distance: 1524.9 km): a – longitudinal sections, b – perpendicular sections: b₁, b₂, b₃, b₄, b₅ – sections in the area of base material, b₆, b₇ – sections in the area of cemented carbide plates.

This is also confirmed by the presence of pinholes on the surfaces of the base material of the coulters (Figs. 18 and 23), owing to the large and hard soil particles.

CONCLUSIONS

The tested coulters (A/1 and B) were characterised by a similar *uznich* characterised by the highest intensity of wear (especially the B coulters installed on the first cultivator beam), in spite of their reinforcement by cemented carbide plates that formed blades. This indicates high load of the cutting edge of the elements, where the material is worn by soil, as well as from the sides of the flank face and the rake face. The most width reduction of the elements occurred in the area located directly behind the cemented-carbide plates and in the area of their brazing. However, the most thickness reduction of the coulters occurred in the base material area, which was particularly noticeable in the B coulters reinforced only with cemented-carbide plates. The amount of length, width, and thickness reduction was the highest for the coulters on the first cultivator beam and was lower for the elements installed on the subsequent beams.

1. The basic form of wear of the cemented-carbide plates was removal of the matrix by fine fraction of soil, leading to weaker mounting of carbide grains, followed by cracking, crushing or chipping of the grains due to the action of larger soil particles. Padding welds were subjected to a complex mechanism of abrasive wear, including delamination of the material, microcutting, and grooving. Such a course of wear of the padding welds was related to their irregular, multilayer microstructure. The dominant wear mechanism of the

steel with microaddition of boron was grooving and microcutting.

2. Cemented carbide plates, which formed the blade of the coulters, were subjected to crushing on the edges, resulting in a rapid length reduction. Thus, crushing of the plates (due to the presence of stones in the cultivated soils) can affect the durability of the elements.
3. The coulters were subjected to various mechanisms and intensities of wear. With regard to the unit thickness reduction, the cemented carbide plates were characterised by the highest resistance to wear. However, the material subjected to the most intensive wear was the base material.

The use of padding welds (A/1 coulters) resulted in improved abrasive-wear resistance, as demonstrated by the lower rate of thickness and width reduction in relation to B coulters, in which this form of reinforcement did not occur.

4. The surfaces of the cemented-carbide plates and the padding welds were characterised by higher roughness than the surface of the less abrasive-wear-resistant base material of the coulters. This means that, in the present research, the roughness measurements of the working surfaces of the coulters should not be connected with the intensity of the destruction process but with the mechanism of this process.

5. The A/1 coulters were already tested in previous field research carried out under different soil conditions. The results of those tests and our results indicate that, depending on the tillage conditions, abrasive wear causes various geometrical changes of the elements. This indicates that further field research is necessary for objective evaluation of the practical usefulness of tools working in soil, especially when they are built of materials with different resistance to abrasive wear.

6.

ACKNOWLEDGEMENTS

Special thanks to Dr. Grzegorz Pękalski from the Faculty of Mechanical Engineering (Wrocław University of Science and Technology) for his invaluable discussion about the wear mechanisms and microstructure analysis.

REFERENCES

- [1] G. Barzegari, A. Uromeihy, J. Zhao, Parametric study of soil abrasivity for predicting wear issue in TBM tunneling projects, *Tunn. Undergr. Space Technol.* 48(2015) 43–57.
- [2] J.M. Fielke, Interactions of the cutting edge of tillage implements with soil, *J. Agric. Eng. Res.* 63 (1996) 61–72.
- [3] P. Hrabec, M. Müller, Research of overlays influence on plough share lifetime, *Res. resistance to abrasive wear. The length reduction of the coulters was* *Agric. Eng. Inf. Process. Agric.* 59 (4) (2013) 147–152.
- [4] P. Kostencki, R. Nowowiejski, Wytrzymałość cierna w wybranych chlemisszy podczas uprawy pługowej z kłód w chstach na wilgocenie, *Tribologia* 2(2006) 123–142.
- [5] P. Kostencki, Geometria zużycia lemieszki pługowej w glebach piaszczystych, *Problemy Inżynierii Rolniczej* 3(57)(2007) 49–64.
- [6] M. Mosleh, E.A. Gharahbagh, J. Rostami, Effects of relative hardness and moisture on tool wear in soil excavation operations, *Wear* 302(2013) 1555–1559.
- [7] E.A. Miller, Wear in tillage tools, in: M.D. Peterson, W.O. Winer (Eds.), *Wear Control Handbook*, ASME, New York, 1984, pp. 987–998.
- [8] J. Napiórkowski, Wpływ do czynników intensywne zużycia elementów roboczych, *Tribologia* 5–6 (1997) 793–801.
- [9] J. Napiórkowski, K. Kolakowski, A. Pergol, Ocena zużycia nowoczesnych materiałów konstrukcyjnych stosowanych narzędzi obrabiających glebę, *Inżynieria Rolnicza* 5(130)(2011) 191–197.
- [10] A. Natsis, G. Papadakis, J. Pitsilis, The influence of soil type, soil water and share sharpness of a mouldboard plough on energy consumption, rate of work and tillage quality, *J. Agric. Eng. Res.* 72 (1999) 171–176.
- [11] A. Natsis, G. Petropoulos, C. Pandazaras, Influence of local soil conditions on mouldboard plough share abrasive wear, *Tribol. Int.* 41(2008) 151–157.
- [12] Z. Owsiak, Wear of spring tine cultivator points in sandy loam and light clay soils in southern Poland, *Soil Tillage Res.* 50(1999) 333–340.
- [13] M.G. Hamblin, G.W. Stachowiak, Description of abrasive particle shape and its relation to two-body abrasive wear, *Tribol. Trans.* 39 (1996) 803–810.
- [14] J. Napiórkowski, Zużycie oddziaływanie gleby na elementy robocze narzędzi rolniczych, *Inżynieria Rolnicza* 9(2005) 3–171.
- [15] A.K. Bhakat, A.K. Mishra, N.S. Mishra, S. Jha, Metallurgical life cycle assessment through prediction of wear for agricultural grade steel, *Wear* 257 (2004) 338–346.

- [16] B. Białoźrzaska, P. Kostencki, Abrasive wear characteristics of selected low-alloy boron steels as measured in both field experiments and laboratory tests, *Wear* 328–329 (2015) 149–159.
- [17] U. Er, B. Par, Wear of plowshare components in SAE 950C steel surface hardened by powder boriding, *Wear* 261(3–4)(2006)251–255.
- [18] Z. Tian, W. Sun, M. Shang, X. Jiang, W. Han, L. Li, Application of boronizing technology on plowshares and study on the abrasive wear characteristics under low stress of boronized layer, in: *Proceedings of the International Symposium on Agricultural Engineering (89-ISAIE)*, Beijing, China, 12–15 September 1989, International Academic Publishers, Beijing, China, 1989, pp. 248–249.
- [19] Y. Bayhan, Reduction of wear via hardfacing of chisel plowshare, *Tribol. Int.* 39 (6) (2006) 570–574.
- [20] D. Bartkowski, G. Kinal, B. Dudziak, A. Piasecki, W. Matysiak, Microstructure and wear resistance of steel-6/wc metal matrix composite coatings, *J. Res. Appl. Agric. Eng.* 60 (2) (2015) 21–25.
- [21] Z. Horvat, D. Filipovic, S. Kosutic, R. Emert, Reduction of mouldboard plow share wear by a combination technique of hardfacing, *Tribol. Int.* 41 (8 August) (2008) 778–782.
- [22] P. Novák, M. Müller, P. Hrabec, Research of a material and structural solution in the area of conventional soil processing, *Agron. Res.* 12(1)(2014)143–150.
- [23] J. Zhang, R. L. Kushwaha, Wear and draft of cultivator sweeps with hardened edges, *Can. Agric. Eng.* 37 (1) (1995) 41–47.
- [24] J. Napiórkowski, K. Ligier, G. Pękalski, Właściwości tribologiczne węglika w spiekanych w glebowej masie czarnej, *Tribologia* 2(2014)123–134.
- [25] P. Kostencki, T. Stawicki, B. Białoźrzaska, Durability and wear geometry of subsoiler shanks provided with sintered carbide plates, *Tribol. Int.* 104 (2016) 19–35.
- [26] T. Stawicki, P. Kostencki, B. Białoźrzaska, Wear resistance of selected cultivator coulters reinforced with sintered-carbide plates, *Archives of Civil and Mechanical Engineering* 18 (4) (2018) 1661–1678.
- [27] A.G. Foley, P.J. Lawton, A.W. Barker, V.A. McLees, The use of alumina ceramic to reduce wear of soil-engaging components, *J. Agric. Eng. Res.* 30(1984)37–46.
- [28] A.G. Foley, C.J. Chisholm, V.A. McLees, Wear of ceramic-protected agricultural subsoilers, *Tribol. Int.* 21 (2) (1988) 97–103.
- [29] J. Napiórkowski, K. Ligier, Wear testing of Al₂O₃ oxide ceramic in a diverse abrasive soil mass, *Tribologia* 1 (2014) 63–74.
- [30] M. Ucgul, J. M. Fielke, Ch Saunders, Defining the effect of sweep tillage tool cutting edge geometry on tillage forces using 3D discrete element modeling, *Information Processing in Agriculture 2* (2015) 130–141.
- [31] A. Khalilian, Y. J. Han, M. W. Marshall, S. Gorucu, Y. Abbaspour-Gilandeh, K. R. Kirk, Evaluation of the Clemson instrumented subsoiler shank in coastal plain soils, *Comput. Electron. Agric.* 109 (2014) 46–51.
- [32] Ch Hang, X. Gao, M. Yuan, Y. Huang, R. Zhu, Discrete element simulations and experiments of soil disturbance as affected by the tine spacing of subsoiler, *Biosyst. Eng.* 168 (2018) 73–82.
- [33] S. Karmakar, R. Lal Kushwaha, Dynamic modeling of soil-tool interaction: an overview from a fluid flow perspective, *J. Terramechanics* 43 (2006) 411–425.
- [34] I. Shmulevich, State of the art modeling of soil-tillage interaction using discrete element method, *Soil Tillage Res.* 111(2010)41–53.
- [35] L. Zhu, J. R. Ge, X. Cheng, S. S. Peng, Y. Y. Qi, W. F. Zhang, D. Q. Zhu, Modeling of share/soil interaction of a horizontally reversible plow using computational fluid dynamics, *J. Terramechanics* 72 (2017) 1–8.
- [36] L. Zhu, X. Cheng, S. S. Peng, Y. Y. Qi, W. F. Zhang, R. Jiang, C. L. Yin, Three dimensional computational fluid dynamic interaction between soil and plow breast of horizontally reversal plow, *Comput. Electron. Agric.* 123 (2016) 1–9.
- [37] M. Kirchgaßner, E. Badisch, F. Franek, Behaviour of iron-based hardfacing alloys under abrasion and impact, *Wear* 265 (2008) 772–779.
- [38] V. Jankauskas, M. Antonov, V. Varnauskas, R. Skirkus, D. Goljandin, Effect of WC grain size and content on low stress abrasive wear of manual arc welded hardfacings with low-carbon or stainless steel matrix, *Wear* 328–329 (2015) 378–390.
- [39] S. Chatterjee, T. K. Pal, Wear behaviour of hardfacing deposits on cast iron, *Wear* 255 (2003) 417–425.
- [40] F. Bosio, E. Bassini, C. G. Orta Salazar, D. Ugues, D. Peila, The influence of microstructure on abrasive wear resistance of selected cemented carbide grades operating as cutting tools in dry and foam conditioned

- soil, *Wear* 394–395 (2018)203–216.
- [41] M.G. Gee, A. Gant, B. Roebuck, Wear mechanisms in abrasion and erosion of WC/Co and related hardmetals, *Wear* 263(2007)137–148.
- [42] H. Saito, A. Iwabuchi, T. Shimizu, Effects of Co content and WC grain size on wear of WC cemented carbide, *Wear* 261 (2006) 126–132.
- [43] C. Allen, M. Sheen, J. Williams, V. A. Pugsley, The wear of ultrafine WC–Co hardmetal, *Wear* 250 (2001) 604–610.
- [44] M.G. Gee, A. Gant, B. Roebuck, Wear mechanisms in abrasion and erosion of WC/Co and related hardmetals, *Wear* 263(2007)137–148.
- [45] A.J. Gant, M.G. Gee, B. Roebuck, Rotating wheel abrasion of WC/Co hardmetals, *Wear* 258 (2005)178–188.
- [46] T.A. Adler, O.N. Dogan, Erosive wear and impact damage of high-chromium white cast irons, *Wear* 229 (1999)174–180.
- [47] A.N.J. Stevenson, I.M. Hutchings, Wear of hardfacing white cast irons by solid particle erosion, *Wear* 186 (1995)150–158.
- [48] O.N. Dogan, J.A. Hawk, G. Laird, Solidification structure and abrasion resistance of high chromium white irons, *Metall. Mater. Trans. A: Phys. Metall. Mater. Sci.* 28(1997) 1315–1328.
- [49] Jibo Wang, Tiantian Li, Yefei Zhou, Xiaolei Xing, Sha Li, Yulin Yang, Qingxiang Yang, Effect of nitrogen alloying on the microstructure and abrasive impact wear resistance of Fe-Cr-C-Ti-Nb hardfacing alloy, *Surf. Coat. Technol.* 309(15 January) (2017) 1072–1080.
- [50] R.J. Chung, X. Tang, D.Y. Li, B. Hinckley, K. Dolman, Microstructure refinement of hypereutectic high Cr cast irons using hard carbide-forming elements for improved wear resistance, *Wear* 301 (2013)695–706.